Using Electrical Energy Storage to Mitigate Natural Gas-Supply Shortages

Bining Zhao, *Student Member, IEEE,* Antonio J. Conejo, *Fellow, IEEE,* and Ramteen Sioshansi, *Senior Member, IEEE*

***Abstract*—The recent leak of the Aliso Canyon natural gas-storage facility calls for co-ordinated planning of natural gas and electric power systems with specific consideration of electrical energy storage. This paper proposes a co-ordinated planning model that fills this need. The model is formulated as a two-stage stochastic optimization problem, in which electricity- and natural gas-demand-growth and natural gas-supply uncertainties are represented. We analyze the trade-off between building electrical, natural gas, and electrical energy storage infrastructure. The sensitivity of electrical energy storage investment to the modeling of the operating conditions is also studied. The model is tested using a California-based case study.**

***Index Terms*—Power system planning, natural gas, energy storage, stochastic optimization**

I. Introduction

ELECTRIC power systems are becoming increasingly reliant on natural gas systems, due to the greater use of natural gas-fired generation. This dependency can increase the brittleness of electricity systems. Southern California is currently experiencing this as a result of a leak at the Aliso Canyon natural gas-storage facility, which was discovered in late 2015. As of late 2017, the facility can still be operated only during emergencies and at greatly reduced capacity.[1] As a result, Southern California Gas Company (SoCalGas) is operating with a 64% loss of natural gas inventory and a 51% loss of natural gas-withdrawal capacity. In addition to affecting the ability of SoCalGas to serve industrial and residential natural gas demands, the limited fuel supply also affects 17 natural gas-fired generating units in southern California. These units represent more than 70% of the local generating capacity. To deal with the limited local fuel supply, that California Public Utilities Commission (CPUC) authorized, via Resolution E-4791, expedited procurement of electrical energy storage (EES) by Southern California Edison (SCE). SCE procured 62 MW of EES capacity in 2016, with further procurements expected in 2017.

Within this context, this paper proposes an integrated model to co-optimize the expansion of EES, in conjunction with electrical and natural gas infrastructures, to reliably supply electric loads at least cost. The purpose of this work is to investigate the role of EES in mitigating fuel-supply shortages for natural gas-fired units. Our proposed model is formulated as a two-stage stochastic optimization problem, in which investment decisions are made in the first stage, followed by a variety of operating conditions under different potential random scenarios. Scenarios can represent uncertainties around electricity- or natural gas-demand growth, and in natural gas supply (*i.e.*, representing an Aliso Canyon-like event). We apply our model to a simple example and a more comprehensive California-based case study. We use these to analyze the trade-offs between building electrical, EES, and natural gas facilities.

To our knowledge the extant literature does not provide a modeling framework that can co-optimize the expansion of electric and natural gas systems, while explicitly accounting for EES. Our previous work [1] develops a modeling framework for co-ordinated expansion planning of electric and natural gas systems without EES. This paper builds off of our previous work by explicitly including EES, allowing it to serve as an alternative to having to reinforce electric or natural gas systems. Such a model would be of immense value as power system operators, policy makers, and regulators are increasingly having to manage supply shortages, such as the one that is affecting California today. The inclusion of EES requires some non-trivial changes to the structure of our planning model, such as attention to the representation of operating periods. These details are explored in depth in the example and case study that are presented herein.

The remainder of this paper is organized as follows. Section II surveys the existing literature and discusses our contribution. Section III provides a detailed formulation of the proposed planning model. Section IV illustrates the model through a simple example, while Section V analyzes a California-based case study. Section VI concludes.

II. Literature Review

EES-capacity planning has evolved as the role of EES has grown. EES was initially seen as an alternative to utilities' building peaking generation in their integrated resource planning [2]. More recent work [3] recognizes novel uses of EES beyond alleviating generation-capacity constraints. One body of work [4]–[9] examines the use of EES to integrate wind generation, by accommodating the variability and uncertainty

This work was supported by NSF grant 1548015.

B. Zhao is with the Department of Electrical and Computer Engineering, The Ohio State University, Columbus, OH 43210, USA (e-mail: zhao.1418@osu.edu).

A. J. Conejo is with the Department of Integrated Systems Engineering and the Department of Electrical and Computer Engineering, The Ohio State University, Columbus, OH 43210, USA (e-mail: conejonavarro.1@osu.edu).

R. Sioshansi is with the Department of Integrated Systems Engineering, The Ohio State University, Columbus, OH 43210, USA (e-mail: sioshansi.1@osu.edu).

[1]The California Public Utilities Commission has a public docket related to the Aliso Canyon failure, which is available at: http://www.cpuc.ca.gov/Aliso

of its real-time availability. A second research area [10], [11] models EES investment to maximize the value streams that it can derive from wholesale-market prices. A third body of work models the deployment of EES at the distribution level [8], [12] and within microgrids [9], [13].

EES can also be used toward other industrial applications that are outside of the power system realm. Anvari-Moghaddam *et al*. [14] and Clerici *et al*. [15] discuss the use of EES in ships and railways, respectively. Lachuriya and Kulkarni [16] and Zou *et al*. [17] survey the potential use of different EES technologies in industrial applications.

Co-ordinated planning of electric power and natural gas systems takes numerous approaches. Some works [18]–[21] employ multistage deterministic models. Unsihuay-Vila *et al*. [18] employ a linear model while Qiu *et al*. [19] and Barati *et al*. [20] employ nonlinear models that are solved using metaheuristic algorithms. Zeng *et al*. [21] develop a bi-level planning model that is solved using metaheuristic algorithms. Other works take account of uncertainty to enhance the reliability of planning decisions, *e.g*., via multistage stochastic optimization [22], robust optimization that includes $N-1$ and probabilistic reliability criteria [23], or multi-objective optimization that accounts for $N-1$ criteria [24]. Qiu *et al*. [25] employ Taylor series approximations and piecewise-linear functions to linearize the nonlinear characteristics of natural gas systems. Other works [26], [27] use natural gas-transportation models for co-planning of the two systems to enhance security and resilience. Another body of work [28], [29] co-optimizes electric and natural gas systems with the aim of reducing carbon emissions.

The existing literature has an important gap that this paper seeks to fill. Namely, there are no works (to our knowledge) that tackle the joint expansion planning of EES, natural gas, and power systems. Instead, existing works treat these as separate problems. Given the role that EES can play in mitigating the brittleness of electricity supply in light of natural gas-supply disruptions, the model that we propose addresses a timely and important issue. Our work makes three major contributions to the existing literature. First, we propose a two-stage stochastic optimization model, which shows that EES is a viable alternative to expanding other (*e.g*., electric or natural gas infrastructures) to mitigate fuel shortages or other supply issues. Second, we study the impact of the representation of operating conditions on EES-investment decisions. This expands upon other works [30] that show the impacts of representing operating constraints on EES investments. Finally, we use a California-based case study to test the proposed model. In doing so, we demonstrate the benefits of EES in alleviating fuel-supply shortages in a real-world setting.

III. Model Formulation

A. Model Notation

Sets and Indices

c	index of candidate thermal units in set, Φ^{TC}
e	index of existing thermal units in set, Φ^{TE}
g	index of candidate natural gas-fired units in set, Φ^{GC}
i	index of candidate EES units in set, Φ^{SC}
j	index of existing EES units in set, Φ^{SE}
k	index of existing natural gas-fired units in set, Φ^{GE}
m, n	indices of power system nodes in set, Λ
o	index of operating conditions in set, O
p, q	indices of natural gas system nodes in set, Ξ
t	index of hours in each operating condition in set, T
Λ_n	set of nodes directly connected to node n through existing transmission lines
$\hat{\Lambda}_n$	set of nodes directly connected to node n through candidate transmission lines
Ξ_p	set of nodes directly connected to node p through existing pipelines
$\hat{\Xi}_p$	set of nodes directly connected to node p through candidate pipelines
Ξ_p^{GC}	set of candidate natural gas-fired units connected to natural gas system node p
Ξ_p^{GE}	set of existing natural gas-fired units connected to natural gas system node p
Φ_n^{GC}	set of candidate natural gas-fired units located at power system node n
Φ_n^{GE}	set of existing natural gas-fired units located at power system node n
Φ_n^{SC}	set of candidate EES units located at node n
Φ_n^{SE}	set of existing EES units located at node n
Φ_n^{TC}	set of candidate thermal units located at node n
Φ_n^{TE}	set of existing thermal units located at node n
ω	index of scenarios in set, Ω

Parameters

b_g^{GC}	heat rate of candidate natural gas-fired unit g [MBTU/MWh]
b_k^{GE}	heat rate of existing natural gas-fired unit k [MBTU/MWh]
$B_{m,n}$	susceptance of existing transmission line connecting nodes m and n [S]
$\hat{B}_{m,n}$	susceptance of candidate transmission line connecting nodes m and n [S]
$C_c^{\mathrm{T,INV}}$	investment cost of candidate thermal unit c [$/MW]
$C_g^{\mathrm{G,INV}}$	investment cost of candidate natural gas-fired unit g [$/MW]
$C_i^{\mathrm{S,INV}}$	investment cost of candidate EES unit i [$/MW]
$C_{m,n}^{\mathrm{E,INV}}$	investment cost of candidate transmission line connecting nodes m and n [$]
$C_{p,q}^{\mathrm{G,INV}}$	investment cost of candidate pipeline connecting nodes p and q [$/MBTU/h]
$D_i^{\mathrm{SC,max}}$	discharging capacity of candidate EES unit i [MW]
$D_j^{\mathrm{SE,max}}$	discharging capacity of existing EES unit j [MW]
$f_{\omega,o,t}^{\mathrm{E}}$	hour-t electric load in operating condition o of scenario ω [p.u.]
$f_{\omega,o,t}^{\mathrm{G}}$	hour-t non-generation-related natural gas load in operating condition o of scenario ω [p.u.]
$f_{\omega,o,t}^{\mathrm{GS}}$	hour-t natural gas supply available in operating condition o of scenario ω [p.u.]
$F_{m,n}^{\max}$	capacity of existing transmission line connecting nodes m and n [MW]

$F^{\mathrm{C,max}}_{m,n}$ capacity of candidate transmission line connecting nodes m and n [MW]
K^{GC}_{g} operation and maintenance cost of candidate natural gas-fired unit g [$/MWh]
K^{GE}_{k} operation and maintenance cost of existing natural gas-fired unit k [$/MWh]
K^{TC}_{c} marginal cost of candidate thermal unit c [$/MWh]
K^{TE}_{e} marginal cost of existing thermal unit e [$/MWh]
L^{E}_{n} reference electric load at node n [MW]
L^{G}_{p} reference non-generation-related natural gas load at node p [MBTU]
M a large constant
$P^{\mathrm{TC,I,max}}_{c}$ maximum capacity of candidate thermal unit c that can be built [MW]
$P^{\mathrm{TC,RD}}_{c}$ ramp-down limit of candidate thermal unit c [MW/h]
$P^{\mathrm{TC,RU}}_{c}$ ramp-up limit of candidate thermal unit c [MW/h]
$P^{\mathrm{TE,max}}_{e}$ capacity of existing thermal unit e [MW]
$P^{\mathrm{TE,RD}}_{e}$ ramp-down limit of existing thermal unit e [MW/h]
$P^{\mathrm{TE,RU}}_{e}$ ramp-up limit of existing thermal unit e [MW/h]
$P^{\mathrm{GC,I,max}}_{g}$ maximum capacity of candidate natural gas-fired unit g that can be built [MW]
$P^{\mathrm{GC,RD}}_{g}$ ramp-down limit of candidate natural gas-fired unit g [MW/h]
$P^{\mathrm{GC,RU}}_{g}$ ramp-up limit of candidate natural gas-fired unit g [MW/h]
$P^{\mathrm{GE,max}}_{k}$ capacity of existing natural gas-fired unit k [MW]
$P^{\mathrm{GE,RD}}_{k}$ ramp-down limit of existing natural gas-fired unit k [MW/h]
$P^{\mathrm{GE,RU}}_{k}$ ramp-up limit of existing natural gas-fired unit k [MW/h]
$Q^{\mathrm{SC,max}}_{i}$ charging capacity of candidate EES unit i [MW]
$Q^{\mathrm{SE,max}}_{j}$ charging capacity of existing EES unit j [MW]
$R^{\mathrm{max}}_{p,q}$ capacity of existing pipeline connecting nodes p and q [MBTU/h]
$R^{\mathrm{I,max}}_{p,q}$ maximum capacity of candidate pipeline connecting nodes p and q that can be built [MBTU/h]
$S^{\mathrm{SC,I,max}}_{i}$ maximum energy capacity of candidate EES unit i that can be built [MWh]
$S^{\mathrm{SE,max}}_{j}$ energy capacity of existing EES unit j [MWh]
V^{E} value of lost electric load [$/MWh]
V^{G} value of lost natural gas load [$/MBTU]
w_o weight of operating condition o
X^{max}_{p} reference natural gas-supply capacity at natural gas system node p [MBTU/h]
$\beta_{p,\omega,o}$ scenario-ω natural gas price at node p in operating condition o [$/MBTU]
η^{SC}_{i} roundtrip efficiency of candidate EES unit i
η^{SE}_{j} roundtrip efficiency of existing EES unit j
θ_{ref} phase angle of reference node [rad]
π_ω probability of scenario ω occurring

Variables

$P^{\mathrm{GC,INV}}_{g}$ capacity of candidate natural gas-fired unit g built [MW]
$P^{\mathrm{TC,INV}}_{c}$ capacity of candidate thermal unit c built [MW]
$\hat{R}^{\mathrm{INV}}_{p,q}$ capacity of candidate pipeline connecting nodes p and q built [MBTU/h]
$S^{\mathrm{SC,INV}}_{i}$ capacity of candidate EES unit i built [MWh]
$x_{m,n}$ binary variable that equals 1 if candidate transmission line connecting nodes m and n is built and equals 0 otherwise
$D^{\mathrm{SC}}_{i,\omega,o,t}$ hour-t discharging of candidate EES unit i in operating condition o of scenario ω [MW]
$D^{\mathrm{SE}}_{j,\omega,o,t}$ hour-t discharging of existing EES unit j in operating condition o of scenario ω [MW]
$F^{\mathrm{C}}_{m,n,\omega,o,t}$ hour-t flow through candidate transmission line connecting nodes m and n in operating condition o of scenario ω [MW]
$L^{\mathrm{shed,E}}_{n,\omega,o,t}$ hour-t unserved electric load at node n in operating condition o of scenario ω [MW]
$L^{\mathrm{shed,G}}_{p,\omega,o,t}$ hour-t unserved natural gas demand at node p in operating condition o of scenario ω [MBTU]
$P^{\mathrm{TC}}_{c,\omega,o,t}$ hour-t production of candidate thermal unit c in operating condition o of scenario ω [MW]
$P^{\mathrm{TE}}_{e,\omega,o,t}$ hour-t production of existing thermal unit e in operating condition o of scenario ω [MW]
$P^{\mathrm{GC}}_{g,\omega,o,t}$ hour-t production of candidate natural gas-fired unit g in operating condition o of scenario ω [MW]
$P^{\mathrm{GE}}_{k,\omega,o,t}$ hour-t production of existing natural gas-fired unit k in operating condition o of scenario ω [MW]
$Q^{\mathrm{SC}}_{i,\omega,o,t}$ hour-t charging of candidate EES unit i in operating condition o of scenario ω [MW]
$Q^{\mathrm{SE}}_{j,\omega,o,t}$ hour-t charging of existing EES unit j in operating condition o of scenario ω [MW]
$R_{p,q,\omega,o,t}$ hour-t flow in existing pipeline connecting nodes p and q in operating condition o of scenario ω [MBTU/h]
$\hat{R}_{p,q,\omega,o,t}$ hour-t flow in candidate pipeline connecting nodes p and q in operating condition o of scenario ω [MBTU/h]
$S^{\mathrm{SC}}_{i,\omega,o,t}$ ending hour-t state of charge (SoC) of candidate EES unit i in operating condition o of scenario ω [MWh]
$S^{\mathrm{SE}}_{j,\omega,o,t}$ ending hour-t SoC of existing EES unit j in operating condition o of scenario ω [MWh]
$U^{\mathrm{GC}}_{g,\omega,o,t}$ hour-t fuel use of candidate natural gas-fired unit g in operating condition o of scenario ω [MBTU]
$U^{\mathrm{GE}}_{k,\omega,o,t}$ hour-t fuel use of existing natural gas-fired unit k in operating condition o of scenario ω [MBTU]
$X_{p,\omega,o,t}$ hour-t natural gas supplied at node p in operating condition o of scenario ω [MBTU]
$\theta_{n,\omega,o,t}$ hour-t phase angle at node n in operating condition o of scenario ω [rad]

B. Optimization Model

We propose a static two-stage stochastic model, in which planning decisions are made in the first stage, followed by operational decisions under different scenarios (ω) and operating conditions (o). Our modeling framework is agnostic to the planning and operating horizon. Our example and case study assume investment and operating decisions over a single representative year. As such, investment costs are annualized to make them comparable to the operating costs. Other optimization horizons can be used, so long as the investment costs are properly scaled. To capture the intertemporal dynamics of EES, we use both representative days and representative weeks in the operating conditions. This can be contrasted with planning models that neglect EES [1], which can use decoupled representative hours to capture operating costs. Our model is formulated as a mixed-integer linear optimization problem, which can be solved by standard commercial solvers (*e.g.*, CPLEX or Gurobi). The model formulation is:

$$\min \sum_{i\in\Phi^{\text{SC}}} C_i^{\text{S,INV}} S_i^{\text{SC,INV}} + \sum_{g\in\Phi^{\text{GC}}} C_g^{\text{G,INV}} P_g^{\text{GC,INV}} \tag{1}$$
$$+ \sum_{c\in\Phi^{\text{TC}}} C_c^{\text{T,INV}} P_c^{\text{TC,INV}} + \sum_{n\in\Lambda, m\in\hat{\Lambda}_n} C_{m,n}^{\text{E,INV}} x_{m,n}$$
$$+ \sum_{q\in\hat{\Xi}_p} C_{p,q}^{\text{G,INV}} \hat{R}_{p,q}^{\text{INV}} + \sum_{\omega\in\Omega, o\in O, t\in T} \pi_\omega w_o \cdot$$
$$\Bigg[\sum_{c\in\Phi^{\text{TC}}} K_c^{\text{TC}} P_{c,\omega,o,t}^{\text{TC}} + \sum_{e\in\Phi^{\text{TE}}} K_e^{\text{TE}} P_{e,\omega,o,t}^{\text{TE}}$$
$$+ \sum_{g\in\Phi^{\text{GC}}} K_g^{\text{GC}} P_{g,\omega,o,t}^{\text{GC}} + \sum_{k\in\Phi^{\text{GE}}} K_k^{\text{GE}} P_{k,\omega,o,t}^{\text{GE}}$$
$$+ \sum_p \beta_{p,\omega,o} \cdot \left(\sum_{g\in\Xi_p^{\text{GC}}} U_{g,\omega,o,t}^{\text{GC}} + \sum_{k\in\Xi_p^{\text{GE}}} U_{k,\omega,o,t}^{\text{GE}} \right)$$
$$+ \sum_n V^{\text{E}} L_{n,\omega,o,t}^{\text{shed,E}} + \sum_p V^{\text{G}} L_{p,\omega,o,t}^{\text{shed,G}} \Bigg]$$

$$\text{s.t. } 0 \le P_g^{\text{GC,INV}} \le P_g^{\text{GC,I,max}};\ \forall g \in \Phi^{\text{GC}} \tag{2}$$
$$0 \le P_c^{\text{TC,INV}} \le P_c^{\text{TC,I,max}};\ \forall c \in \Phi^{\text{TC}} \tag{3}$$
$$0 \le S_i^{\text{SC,INV}} \le S_i^{\text{SC,I,max}};\ \forall i \in \Phi^{\text{SC}} \tag{4}$$
$$x_{m,n} \in \{0,1\};\ \forall n \in \Lambda, m \in \hat{\Lambda}_n \tag{5}$$
$$0 \le \hat{R}_{p,q}^{\text{INV}} \le R_{p,q}^{\text{I,max}};\ \forall p \in \Xi, q \in \hat{\Xi}_p \tag{6}$$
$$\sum_{g\in\Phi_n^{\text{GC}}} P_{g,\omega,o,t}^{\text{GC}} + \sum_{k\in\Phi_n^{\text{GE}}} P_{k,\omega,o,t}^{\text{GE}} + \sum_{c\in\Phi_n^{\text{TC}}} P_{c,\omega,o,t}^{\text{TC}} \tag{7}$$
$$+ \sum_{e\in\Phi_n^{\text{TE}}} P_{e,\omega,o,t}^{\text{TE}} + \sum_{j\in\Phi_n^{\text{SE}}} \left(D_{j,\omega,o,t}^{\text{SE}} - Q_{j,\omega,o,t}^{\text{SE}}\right)$$
$$+ \sum_{i\in\Phi_n^{\text{SC}}} \left(D_{i,\omega,o,t}^{\text{SC}} - Q_{i,\omega,o,t}^{\text{SC}}\right) - f_{\omega,o,t}^{\text{E}} L_n^{\text{E}} + L_{n,\omega,o,t}^{\text{shed,E}}$$
$$= \sum_{m\in\Lambda_n} B_{m,n} \cdot (\theta_{n,\omega,o,t} - \theta_{m,\omega,o,t})$$
$$+ \sum_{m\in\hat{\Lambda}_n} F_{m,n,\omega,o,t}^{\text{C}};\ \forall n \in \Lambda, \omega \in \Omega, o \in O, t \in T$$
$$- F_{m,n}^{\max} \le B_{m,n} \cdot (\theta_{n,\omega,o,t} - \theta_{m,\omega,o,t}) \le F_{m,n}^{\max}; \tag{8}$$
$$\forall n \in \Lambda, m \in \Lambda_n, \omega \in \Omega, o \in O, t \in T$$
$$- F_{m,n}^{\text{C,max}} x_{m,n} \le F_{m,n,\omega,o,t}^{\text{C}} \le F_{m,n}^{\text{C,max}} x_{m,n}; \tag{9}$$
$$\forall n \in \Lambda, m \in \hat{\Lambda}_n, \omega \in \Omega, o \in O, t \in T$$
$$- M \cdot (1 - x_{m,n}) \le F_{m,n,\omega,o,t}^{\text{C}} \tag{10}$$
$$- \hat{B}_{m,n} \cdot (\theta_{n,\omega,o,t} - \theta_{m,\omega,o,t}) \le M \cdot (1 - x_{m,n});$$
$$\forall n \in \Lambda, m \in \hat{\Lambda}_n, \omega \in \Omega, o \in O, t \in T$$
$$\theta_{N,\omega,o,t} = \theta_{\text{ref}};\ \forall \omega \in \Omega, o \in O, t \in T \tag{11}$$
$$- \pi \le \theta_{n,\omega,o,t} \le \pi;\ \forall n \in \Lambda, \omega \in \Omega, o \in O, t \in T \tag{12}$$
$$0 \le L_{n,\omega,o,t}^{\text{shed,E}} \le f_{\omega,o,t}^{\text{E}} L_n^{\text{E}}; \tag{13}$$
$$\forall n \in \Lambda, \omega \in \Omega, o \in O, t \in T$$
$$0 \le P_{g,\omega,o,t}^{\text{GC}} \le P_g^{\text{GC,INV}}; \tag{14}$$
$$\forall g \in \Phi^{\text{GC}}, \omega \in \Omega, o \in O, t \in T$$
$$0 \le P_{k,\omega,o,t}^{\text{GE}} \le P_k^{\text{GE,max}}; \tag{15}$$
$$\forall k \in \Phi^{\text{GE}}, \omega \in \Omega, o \in O, t \in T$$
$$0 \le P_{c,\omega,o,t}^{\text{TC}} \le P_c^{\text{TC,INV}}; \tag{16}$$
$$\forall c \in \Phi^{\text{TC}}, \omega \in \Omega, o \in O, t \in T$$
$$0 \le P_{e,\omega,o,t}^{\text{TE}} \le P_e^{\text{TE,max}}; \tag{17}$$
$$\forall e \in \Phi^{\text{TE}}, \omega \in \Omega, o \in O, t \in T$$
$$- P_g^{\text{GC,RD}} \le P_{g,\omega,o,t}^{\text{GC}} - P_{g,\omega,o,t-1}^{\text{GC}} \le P_g^{\text{GC,RU}}; \tag{18}$$
$$\forall g \in \Phi^{\text{GC}}, \omega \in \Omega, o \in O, t \in T$$
$$- P_k^{\text{GE,RD}} \le P_{k,\omega,o,t}^{\text{GE}} - P_{k,\omega,o,t-1}^{\text{GE}} \le P_k^{\text{GE,RU}}; \tag{19}$$
$$\forall k \in \Phi^{\text{GE}}, \omega \in \Omega, o \in O, t \in T$$
$$- P_c^{\text{TC,RD}} \le P_{c,\omega,o,t}^{\text{TC}} - P_{c,\omega,o,t-1}^{\text{TC}} \le P_c^{\text{TC,RU}}; \tag{20}$$
$$\forall c \in \Phi^{\text{TC}}, \omega \in \Omega, o \in O, t \in T$$
$$- P_e^{\text{TE,RD}} \le P_{e,\omega,o,t}^{\text{TE}} - P_{e,\omega,o,t-1}^{\text{TE}} \le P_e^{\text{TE,RU}}; \tag{21}$$
$$\forall e \in \Phi^{\text{TE}}, \omega \in \Omega, o \in O, t \in T$$
$$0 \le S_{i,\omega,o,t}^{\text{SC}} \le S_i^{\text{SC,INV}}; \tag{22}$$
$$\forall i \in \Phi^{\text{SC}}, \omega \in \Omega, o \in O, t \in T$$
$$0 \le S_{j,\omega,o,t}^{\text{SE}} \le S_j^{\text{SE,max}}; \tag{23}$$
$$\forall j \in \Phi^{\text{SE}}, \omega \in \Omega, o \in O, t \in T$$
$$0 \le Q_{i,\omega,o,t}^{\text{SC}} \le Q_i^{\text{SC,max}}; \tag{24}$$
$$\forall i \in \Phi^{\text{SC}}, \omega \in \Omega, o \in O, t \in T$$
$$0 \le Q_{j,\omega,o,t}^{\text{SE}} \le Q_j^{\text{SE,max}}; \tag{25}$$
$$\forall j \in \Phi^{\text{SE}}, \omega \in \Omega, o \in O, t \in T$$
$$0 \le D_{i,\omega,o,t}^{\text{SC}} \le D_i^{\text{SC,max}}; \tag{26}$$
$$\forall i \in \Phi^{\text{SC}}, \omega \in \Omega, o \in O, t \in T$$
$$0 \le D_{j,\omega,o,t}^{\text{SE}} \le D_j^{\text{SE,max}}; \tag{27}$$
$$\forall j \in \Phi^{\text{SE}}, \omega \in \Omega, o \in O, t \in T$$
$$S_{i,\omega,o,t}^{\text{SC}} = S_{i,\omega,o,t-1}^{\text{SC}} + \eta_i^{\text{SC}} Q_{i,\omega,o,t}^{\text{SC}} - D_{i,\omega,o,t}^{\text{SC}}; \tag{28}$$
$$\forall i \in \Phi^{\text{SC}}, \omega \in \Omega, o \in O, t \in T$$
$$S_{j,\omega,o,t}^{\text{SE}} = S_{j,\omega,o,t-1}^{\text{SE}} + \eta_j^{\text{SE}} Q_{j,\omega,o,t}^{\text{SE}} - D_{j,\omega,o,t}^{\text{SE}}; \tag{29}$$
$$\forall j \in \Phi^{\text{SE}}, \omega \in \Omega, o \in O, t \in T$$
$$S_{i,\omega,o,0}^{\text{SC}} = 0;\ \forall i \in \Phi^{\text{SC}}, \omega \in \Omega, o \in O \tag{30}$$
$$S_{j,\omega,o,0}^{\text{SE}} = 0;\ \forall j \in \Phi^{\text{SE}}, \omega \in \Omega, o \in O \tag{31}$$
$$X_{p,\omega,o,t} - \sum_{g\in\Xi_p^{\text{GC}}} U_{g,\omega,o,t}^{\text{GC}} - \sum_{k\in\Xi_p^{\text{GE}}} U_{k,\omega,o,t}^{\text{GE}} \tag{32}$$
$$- f_{\omega,o,t}^{\text{G}} L_p^{\text{G}} + L_{p,\omega,o,t}^{\text{shed,G}} = \sum_{q\in\Xi_p} R_{p,q,\omega,o,t}$$

$$+ \sum_{q \in \hat{\Xi}_p} \hat{R}_{p,q,\omega,o,t}; \ \forall p \in \Xi, \omega \in \Omega, o \in O, t \in T$$

$$- R^{\max}_{p,q} \leq R_{p,q,\omega,o,t} \leq R^{\max}_{p,q}; \quad \forall p \in \Xi, q \in \Xi_p, \omega \in \Omega, o \in O, t \in T \tag{33}$$

$$- \hat{R}^{\text{INV}}_{p,q} \leq \hat{R}_{p,q,\omega,o,t} \leq \hat{R}^{\text{INV}}_{p,q}; \quad \forall p \in \Xi, q \in \hat{\Xi}_p, \omega \in \Omega, o \in O, t \in T \tag{34}$$

$$0 \leq X_{p,\omega,o,t} \leq f^{\text{GS}}_{\omega,o,t} X^{\max}_p; \quad \forall p \in \Xi, \omega \in \Omega, o \in O, t \in T \tag{35}$$

$$0 \leq L^{\text{shed,G}}_{p,\omega,o,t} \leq f^{\text{G}}_{\omega,o,t} L^{\text{G}}_p; \quad \forall p \in \Xi, \omega \in \Omega, o \in O, t \in T \tag{36}$$

$$U^{\text{GC}}_{g,\omega,o,t} = b^{\text{GC}}_g P^{\text{GC}}_{g,\omega,o,t}; \quad \forall g \in \Phi^{\text{GC}}, \omega \in \Omega, o \in O, t \in T \tag{37}$$

$$U^{\text{GE}}_{k,\omega,o,t} = b^{\text{GE}}_k P^{\text{GE}}_{k,\omega,o,t}; \quad \forall k \in \Phi^{\text{GE}}, \omega \in \Omega, o \in O, t \in T. \tag{38}$$

Objective function (1) consists of the sum of the investment and expected operation costs. The first five terms in (1) represent costs of investing in the various technologies. These technologies include EES, natural gas-fired power units, other thermal power units, power transmission lines, and natural gas pipelines. EES-sizing decisions can be made with respect to both the energy and power capacities of a system [10], [11]. Other works [12] only model energy-capacity decisions endogenously. To simplify model notation, we take the latter approach in which the power capacity of EES is fixed and assume that the energy capacity is determined endogenously. It is a straightforward extension of our proposed model to endogenize the power capacity of EES.

The final term in (1) represents the probability-weighted operation cost. This is computed by calculating the operating cost (which consists of fuel and non-fuel operating costs of candidate and existing generating units and the cost of any unserved loads) under each scenario and operating condition. The operating cost under scenario ω and operating condition o, which is given by the terms in the square brackets in (1), is multiplied by π_ω (the probability of scenario ω occurring) and w_o (the weight that is assigned to operating condition o). Adding these terms over all scenarios and operating conditions gives the probability-weighted operation cost.

The model has two sets of constraints. Constraints (2)–(6) correspond to the first and constraints (7)–(38) to the second stage. First-stage constraints (2)–(6) impose limits on the amount of capacity that can be built. Constraints (5) impose the binary nature of transmission-planning decisions.

The operating-stage constraints can be broken into three sets. Constraints (7)–(29) pertain to power system operations. Specifically, constraints (7) enforce nodal load balance. Constraints (8)–(10) enforce flow limits on existing and candidate transmission lines, constraints (11) fix the phase angle of reference node N, and constraints (12) impose limits on the phase angles. Constraints (13) limit unserved nodal load to be no greater than nodal demand. Constraints (14)–(17) impose production limits on candidate and existing generating units. Constraints (18)–(21) impose ramping limits on candidate and existing generating units. Constraints (22) and (23) impose SoC limits on candidate and existing EES units. Constraints (24)–(27) impose power limits on charging and discharging of candidate and existing EES units. Constraints (28) and (29) are energy-balance conditions which define the SoC of each EES unit in each hour in terms of its previous SoC and energy added or removed through charging or discharging (net roundtrip efficiency losses). EES units have roundtrip efficiency smaller than unity. Thus, binary variables are not needed to avoid simultaneous charging and discharging of the EES, as doing so would be suboptimal as a result of wasting energy. Constraints (30) and (31) impose our assumption that each EES unit begins each operating condition with an SoC of zero. The types of constraints that we impose on the operation of the EES are common in the EES-modeling literature [10]–[12].

The second set of constraints, (32)–(36), pertain to the operation of the natural gas system. Constraints (32) impose nodal load balance. Constraints (33) and (34) impose flow limits on existing and candidate pipelines. Constraints (35) impose nodal natural gas-supply limits. Constraints (36) limit unserved natural gas load at each node to be no greater than the nodal demand. Our natural gas model employs a transportation-network representation, which is linear. We employ such a simplification for purposes of computational tractability. A nonlinear flow model would result in a mixed-integer nonlinear stochastic optimization problem, which would raise tractability issues.

The final set of constraints, (37) and (38), define natural gas usage of candidate and existing natural gas-fired units. These constraints provide the linkage between the electricity and natural gas systems.

IV. EXAMPLE

This section illustrates our model using a four-node power system that is coupled with a five-node natural gas system.

A. Data

The topology of the power and natural gas systems is shown in Fig. 1. Natural gas-fired units 1–3 connect the two systems. The operating and investment costs of the existing thermal and natural gas-fired generating units, each of which has a 200-MW capacity, are provided in Table I. Up to 200 MW of new candidate units of the same type can be built at each node. A 600-MWh EES unit with a roundtrip efficiency of 0.8 and 500-MW charging and discharging capacities exists at node 4. Up to 10000 MWh of new EES (with the same technical characteristics) can be built at node 4.

TABLE I
GENERATOR CHARACTERISTICS OF THE EXAMPLE IN SECTION IV

Unit	K^{TH}_e	K^{GE}_k	b^{GE}_k	C^{INV}
$e = 1$	65	n/a	n/a	105000
$k = 1$	n/a	1	9	95000
$k = 2$	n/a	2	10	85000
$k = 3$	n/a	2	10	95000

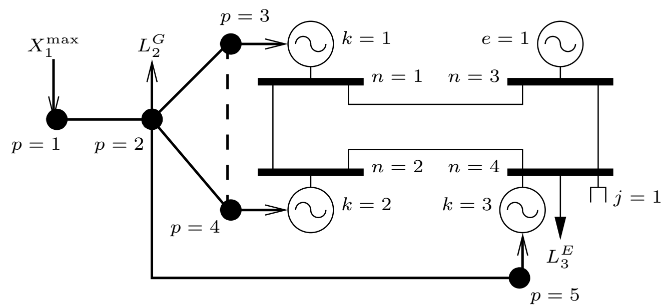

Fig. 1. System topology of the example in Section IV.

The existing transmission lines have capacities of $F_{1,2}^{\max} = F_{1,3}^{\max} = 700$ and $F_{2,4}^{\max} = F_{3,4}^{\max} = 220$. Each of the existing lines can be reinforced with an electrically identical parallel transmission line at a cost of \$11 million per line.

The solid lines in Fig. 1 connecting the natural gas nodes represent existing pipelines, which are assumed to have sufficient capacity to serve all existing natural gas loads except those at node 5. The capacities of existing pipelines can be doubled with expansion costs of $C_{1,2}^{\text{G,INV}} = 750000$, $C_{2,3}^{\text{G,INV}} = C_{2,4}^{\text{G,INV}} = 35000$, and $C_{2,5}^{\text{G,INV}} = 350000$. The dashed line connecting natural gas nodes 3 and 4 represents a nonexistent pipeline that can be built with a maximum capacity of 1500 MBTU/h at a cost of \$35000/MBTU/h.

We model ten operating conditions, and consider cases in which the operating conditions consist of either 24 or 168 hours. This is to determine the impact of the duration of the operating conditions on EES investments. The reference electric and non-generation-related natural gas loads are 707 MW and 3000 MBTU/h, respectively, and the reference natural gas supply is 300000 MBTU/h. Natural gas supply is sufficient to meet non-generation-related demand, thus natural gas curtailment can only occur due to insufficient pipeline capacity. We model five equally likely scenarios in which electric and non-generation-related natural gas demands are scaled by factors 0.8, 0.9, 1.0, 1.1, and 1.2. Thus, there are $10 \times 5 = 50$ operating condition/scenario pairs in total.

B. Results

We first present results for cases in which the model uses 24-hour operating conditions. We then contrast these findings with cases in which the model uses 168-hour (week-long) operating conditions.

1) 24-Hour Operating Conditions: Power system node 4 is a load pocket, which must be served using some combination of transmission, (to import electricity from other nodes), pipeline, (to deliver more fuel to natural gas-fired unit 3), or EES investments. The amounts of pipeline and EES that are built are sensitive to the starting hour of the operating conditions that are modeled. Fig. 2 illustrates this by showing the amounts of EES and pipeline capacities that are built to serve node 4 if different starting hours are used. All other investments remain the same regardless of the starting hour, with 140 MW of capacity added to each of thermal unit 1 and natural gas-fired unit 2, reinforcement transmission lines built connecting node 4 to each of nodes 2 and 3, and 1400 MBTU/h of capacity added to the pipeline connecting nodes 2 and 4.

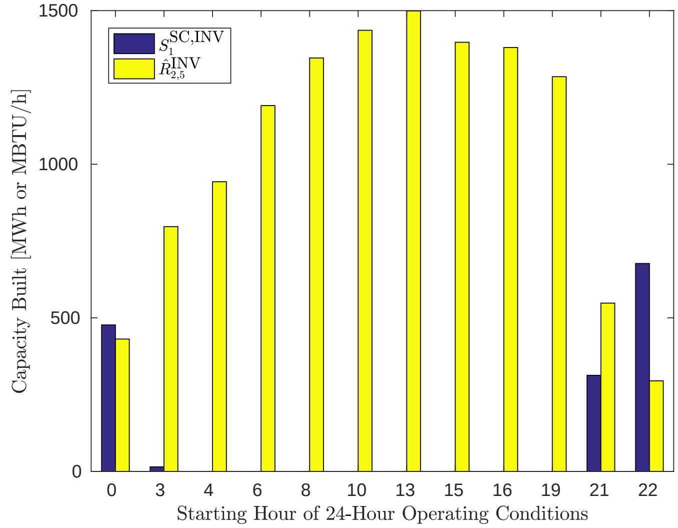

Fig. 2. EES and natural gas-pipeline capacities built with different starting hours for 24-hour operating conditions in the example in Section IV.

The sensitivity of building EES stems from how it alleviates pipeline-capacity needs. This is done by storing excess energy during low-load hours, which is then discharged when loads are higher and the output of natural gas-fired unit 3 is constrained. If the operating conditions modeled begin during high-load hours (*i.e.*, between hours 3 and 19), the load pattern does not appear as being conducive to this use of EES. Conversely, if the operating conditions begin during low-load hours (*i.e.*, between hours 21 and 0), such a use of EES is seen as a viable alternative to building pipeline capacity. For this example, beginning the operating conditions in hour 22 provides the greatest opportunity for using EES to alleviate pipeline-capacity needs. Thus, beginning operating conditions at midnight is not necessarily 'ideal' for capturing these types of benefits of EES. These varying investments also give different expected costs. Starting operating conditions in hour 13 yields the highest costs, which are close to three times the lowest costs that are achieved when starting in hour 22.

2) 168-Hour Operating Conditions: Fig. 3 summarizes EES and pipeline capacities that are built using week-long operating conditions that begin on different days of the week. All of the operating conditions begin at midnight of the respective starting day and all other investments remain the same as in the case with 24-hour operating conditions. Fig. 3 shows that if week-long operating conditions are modeled, there is considerably greater potential for using EES to alleviate pipeline-capacity needs. This is because there is opportunity for inter-day energy shifting, especially between weekends, when loads are relatively low, and weekdays, when loads are relatively high. This inter-day energy shifting also explains the sensitivity of the investment levels to the starting day of the operating conditions. If the week-long operating conditions begin on days with relatively low loads, the load patterns appear more conducive to using EES as an alternative to pipeline capacity. Week-long operating conditions that begin on Wednesday yield the highest expected costs, which are about 35% greater than the lowest expected costs that are achieved with Saturday as the starting day.

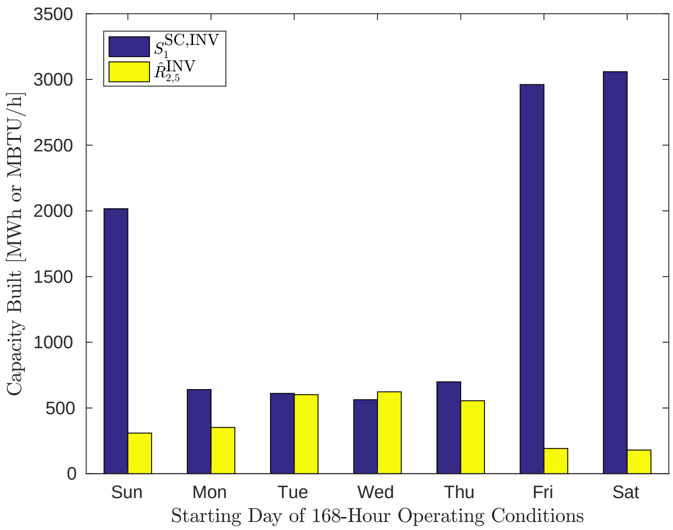

Fig. 3. EES and natural gas-pipeline capacities built with different starting days for 168-hour operating conditions in the example in Section IV.

Combining the results in Figs. 2 and 3 shows that investments in EES are sensitive to all three of the duration, starting hour, and starting day of the operating conditions that are modeled.

C. Computational Details

This example is implemented using version 24.4.6 of the GAMS modeling language and solved using the hybrid branch-and-bound/cutting-plane algorithm with default settings in the CPLEX mixed-integer linear program solver using the NEOS server [31]. The computation times of all of the cases using 24- and 168-hour-long operating conditions are less than 30 minutes. Table II summarizes the sizes of the example problems, in terms of the number of constraints and continuous and binary variables.

TABLE II
SCALE OF OPTIMIZATION PROBLEMS IN THE EXAMPLE IN SECTION IV

Operating Condition Length	Number of Continuous Variables	Number of Binary Variables	Number of Constraints
24 Hours	55215	4	116811
168 Hours	386415	4	822411

V. CALIFORNIA-BASED CASE STUDY

We now present a more detailed case study, which is based on a representation of California and its surrounding region that consists of ten power system and five natural gas nodes. Given that the recent leak that has incapacitated the Aliso Canyon natural gas storage facility is being addressed with the deployment of EES, a California-based case study is of particular real-world relevance.

A. Data

Fig. 4 shows the topology of the electric and natural gas networks. The bars represent power system nodes, which are connected by transmission lines (solid lines). The circles are natural gas nodes, which are connected to one another by pipelines (dashed lines). The dotted arrows pointing out of and into natural gas nodes represent natural gas sinks (*i.e.*, generation- and non-generation-related natural gas demands) and sources, respectively.

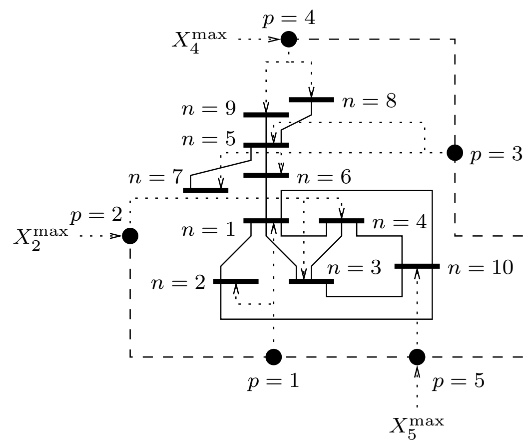

Fig. 4. System topology of the case study in Section V.

Power system nodes 1–4 represent balancing authorities in southern California (SCE, Los Angeles Department of Water and Power, San Diego Gas and Electric, and Imperial Irrigation District, respectively), while nodes 5–7 represent Pacific Gas and Electric's service territory in northern California. Nodes 8–10 represent balancing authorities that are outside of California. Transmission and generator data are obtained from the WECC 2026 Common Case,[2] the California Independent System Operator's (CAISO's) 2016–2017 Transmission Plan, and the CPUC's 2017 Integrated Resource Plan.

The natural gas system is modeled using data that are obtained from the United States Energy Information Administration (EIA).[3] The natural gas source at node 2 represents natural gas-storage facilities other than Aliso Canyon that are located in southern California while the source at node 4 represents natural gas-storage facilities in northern California and supplies from regions that are north of California. The natural gas source at node 5 represents supplies from Nevada, Arizona, and Mexico.

Electric loads are modeled using historical data that are obtained from the Federal Energy Regulatory Commission's (FERC's) Form 714, which are scaled based on the CAISO's 2016–2017 Transmission Plan. Non-generation-related natural gas loads are modeled using historical data that are reported by the EIA.[4] The resulting hourly load data are processed using k-means clustering to generate ten 168-hour operating conditions. The operating condition that is used to represent each resulting cluster is the actual point in the cluster that

[2]https://www.wecc.biz/SystemAdequacyPlanning/Pages/Datasets.aspx
[3]https://www.eia.gov/naturalgas/data.php
[4]https://www.eia.gov/dnav/ng/ng_cons_sum_dcu_nus_a.htm

is closest to its centroid. We also examine the impact of the duration of the operating conditions on investment decisions by dividing each of the ten 168-hour operating conditions that are obtained from the clustering into seven 24-hour operating conditions (yielding 70 day-long operating conditions).

We consider five equally likely scenarios in which all of the electricity and non-generation-related natural gas demands are scaled relative to the reference levels that are obtained from the FERC and EIA data. The scaling factors used are 0.98, 1.00, 1.02, 1.05, and 1.07.

The CAISO's 2016–2017 Transmission Plan reports that the Aliso Canyon leak directly affects 9800 MW of generation in southern California. Thus, the pipeline capacities into natural gas node 1 are set so that there is the equivalent of a 9800-MW fuel shortage during hours with peak natural gas demands.

Based on data that are reported by the EIA,[5] [6] existing generators at power system node 9 have higher operating costs compared to existing units that are at other nodes. We allow up to 2000 MW of new natural gas-fired and thermal units to be built at each node. New natural gas-fired units in all nodes have the same costs of $K_g^{\mathrm{GC}} = 1$ and $b_g^{\mathrm{GC}} = 7.8$, whereas new thermal units in California have lower operating costs. Specifically, $K_c^{\mathrm{TC}} = 25$ for new thermal units at nodes 1–7 and $K_c^{\mathrm{TC}} = 36$ for candidate units in nodes 8–10.

We examine six cases with different generation unit- and pipeline-investment costs. Generation unit-investment costs are summarized in Table III. We allow up to 100000 MBTU/h of new capacity to be added to the existing pipelines serving the Los Angeles basin (*i.e.*, to the pipelines connecting natural gas node 1 to nodes 2 and 5). Pipeline-investment costs are \$20000/MBTU/h in Cases 1 and 4, \$50000/MBTU/h in Cases 2 and 5, and \$500000/MBTU/h in Cases 3 and 6. A single parallel and electrically identical transmission line can be built alongside any existing line. A new line between northern (node 6) and southern (node 1) California or crossing state lines (into nodes 8–10) cost \$20 million each. Remaining lines within the state of California cost \$9.5 million.

TABLE III
INVESTMENT COSTS OF CANDIDATE GENERATING UNITS IN THE EXAMPLE IN SECTION V

	Cases 1–3		Cases 4–6	
n	$C_c^{\mathrm{T,INV}}$	$C_g^{\mathrm{G,INV}}$	$C_c^{\mathrm{T,INV}}$	$C_g^{\mathrm{G,INV}}$
1–7	2921000	696000	2921000	1096000
8–10	796000	696000	1296000	1096000

There is an existing 50-MWh/65-MW EES unit with a roundtrip efficiency of 0.8 at power system node 1. Up to 10000 MWh of new EES with a power capacity of 1500 MW and a roundtrip efficiency of 0.9 can be built at node 1. The EES-investment cost is \$400000/MWh in Cases 1–3 and \$350000/MWh in Cases 4–6.

[5]https://www.eia.gov/naturalgas/data.php#prices
[6]https://www.eia.gov/electricity/annual/html/epa_08_04.html

B. Results

We first present results using 24-hour operating conditions and then discuss the impact on investment decisions of using 168-hour operating conditions.

1) 24-hour Operating Conditions: Table IV summarizes the investments that are made in the six cases using midnight as the starting hour of the operating conditions. In addition to the components listed in the table, transmission lines connecting node 5 to nodes 6 and 9 and a third line connecting nodes 6 and 1 are built in all six cases. Contrasting pipeline investments between the three pairs of Cases 1 and 4, 2 and 5, and 3 and 6 shows that increasing the pipeline-investment cost results in progressively less pipeline capacity being built to alleviate the fuel shortage at natural gas node 1.

TABLE IV
INVESTMENTS MADE WITH 24-HOUR OPERATING CONDITIONS BEGINNING AT MIDNIGHT IN THE CASE STUDY IN SECTION V

	Case					
Component	1	2	3	4	5	6
Node-8 Natural Gas-Fired Unit	0	0	81	0	0	79
Node-10 Natural Gas-Fired Unit	0	0	1998	0	0	1355
Node-1 Energy Storage Unit	0	855	855	0	855	2252
Nodes-1 $\leftrightarrow$ 5 Pipeline	24060	17046	0	24060	17046	0

As the pipeline cost increases, the fuel shortage in southern California is alleviated in varying ways in the different cases. Generating unit-investment costs are higher in Cases 4–6 *vis-à-vis* Cases 1–3, whereas the trend in EES-investment costs is reversed amongst these cases. Thus, more EES and less generating capacity are built in Case 6 *vis-à-vis* Case 3. However, all investments in Cases 1 and 4 are identical, as are those in Cases 2 and 5. Investments are the same in Cases 1 and 4 because the relatively low pipeline-investment cost results in the fuel shortage being mainly alleviated by new pipelines. Cases 2 and 5 have moderate pipeline-investment costs, and as such the fuel shortage is alleviated using a combination of pipelines and EES.

The optimal set of investments in this case study are insensitive to the starting hour of the day-long operating conditions, unless the operating conditions begin between hours 14 and 16. Table V summarizes the investments that are made in Cases 2 and 3 with these hours as the starting hour. There are also transmission lines connecting node 1 to 6 and 5 to 9 that are built in both cases with starting hours between hours 14 and 16. The table shows that if hours 15 or 16 are used as the starting hour, no EES capacity is added. This is because some of the operating conditions have severe pipeline congestion into natural gas node 1 between hours 14 and 16. When hours 15 or 16 are used as the starting hour, the load patterns require more generation capacity to be built at power system nodes 5, 8, and 10 to serve electric loads in southern California, making EES investment uneconomic (because generation capacity must be built regardless of EES investments).

TABLE V
INVESTMENTS MADE WITH 24-HOUR OPERATING CONDITIONS WITH DIFFERENT STARTING HOURS IN THE CASE STUDY IN SECTION V

	Case 2		Case 3	
Component	Hour 14	Hours 15 or 16	Hour 14	Hours 15 or 16
Node-5 Natural Gas-Fired Unit	0	0	461	844
Node-8 Natural Gas-Fired Unit	0	0	98	140
Node-10 Natural Gas-Fired Unit	0	0	2000	2000
Node-1 Energy Storage Unit	376	0	376	0
Nodes-5 $\leftrightarrow$ 6 Transmission Line	Yes	Yes	Yes	No
Nodes-1 $\leftrightarrow$ 5 Pipeline	20980	24470	0	0

A transmission line connecting nodes 5 and 6 is not built in Case 3 if hours 15 or 16 are the starting hour. This is the result of the natural gas-fired unit that is built at node 5. This unit mitigates congestion on the existing line connecting nodes 5 and 6, alleviating the need for a reinforcement line. There is also more capacity added to the pipeline connecting nodes 1 and 5 in Case 2 when the starting hour is 15:00 or 16:00 relative to Case 1 with midnight as the starting hour (which has the lowest pipeline-investment cost). This is because in Case 1 with midnight as the starting hour, existing and new EES units are discharged at 16:00 in some operating conditions. These EES units cannot be discharged during the same hours if 15:00 or 16:00 is the starting hour, requiring more pipeline capacity to accommodate electric loads.

There are 70 day-long operating conditions in each scenario in all of the six cases that are examined. To verify that this number of operating conditions gives a good representation of the full year, we examine the optimal objective-function value and investments that are made with different numbers of operating conditions. Fig. 5 summarizes the optimal objective-function value if between 68 and 80 days are used to represent the operating conditions of the year (these days are obtained using the same k-means clustering technique that is described in Section V-A). The figure shows that the optimal objective-function has very little variability as the number of operating days is changed (the optimal objective-function values that are obtained are within 0.3% of one another). The optimal investments similarly show very little change with different numbers of representative operating days. These results suggest that 70 operating days provide a sufficiently rich mix of load and supply conditions to accurately represent the full year.

2) 168-Hour Operating Conditions: The results are identical if 168-hour operating conditions are used to those that are obtained with 24-hour operating conditions. Indeed, the investment are identical even if the starting day of the week-long operating conditions are changed. This stems from the load profile and generation mix of the system. Most hours with low electric loads result in lower-cost generating units being fully loaded. As such, EES has a limited role to play in storing lower-cost energy to displace higher-cost units during

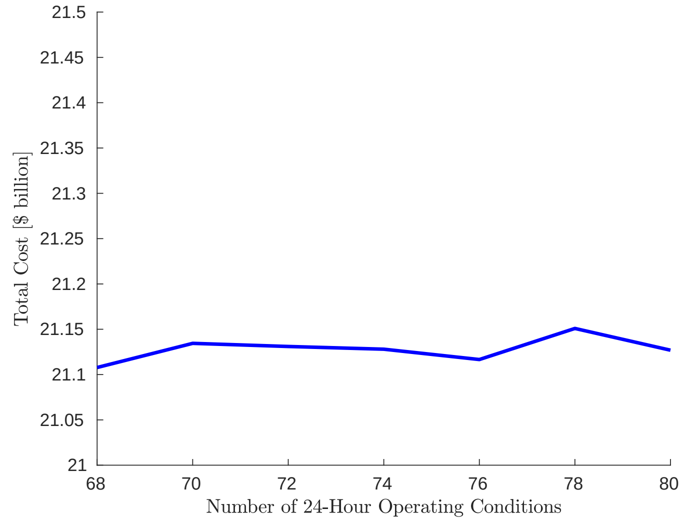

Fig. 5. Optimal objective-function value with different numbers of day-long operating conditions in the case study in Section V.

hours with high electric loads. Instead, EES is built solely to mitigate the fuel shortage in southern California. Subject to using the correct starting hour, day-long operating conditions capture this use of EES. Thus, week-long operating conditions provide no added planning benefit in this particular case study. However, this result would not stand in a system or case study with different generation-cost structures or load profiles.

C. Computational Details

This case study is implemented using version 24.4.6 of the GAMS modeling language and solved using the hybrid branch-and-bound/cutting-plane algorithm with default settings in the CPLEX mixed-integer linear program solver on the NEOS server [31]. The computation times of all cases using day- and week-long operating conditions are less than one hour. Table VI summarizes the scales of the optimization problems in the case study that model 70 day-long and 10 week-long operation conditions, in terms of the number of constraints and continuous and binary variables.

TABLE VI
SCALE OF OPTIMIZATION PROBLEMS IN THE CASE STUDY IN SECTION V

Operating Condition Length	Number of Continuous Variables	Number of Binary Variables	Number of Constraints
24 Hours	1898439	13	4325326
168 Hours	1898439	13	4325326

VI. CONCLUSION

The recent failure of the Aliso Canyon natural gas-storage facility raises the need to jointly plan natural gas and electric power systems, with consideration of EES. This paper provides a model that allows co-ordinating such planning, under uncertainties in electricity- and natural gas-demand growth and natural gas supply. The case study results show that EES is a viable alternative to building natural gas or 'traditional' electrical units. The sensitivity of EES investment to the modeling of operating conditions is studied. Using week- as opposed to day-long operating conditions may result in different investments, as can the choice of the starting hour of day of operating conditions. These impacts depend, however, on the specific load patterns and technology mix of the system.

Our work focuses on EES as a means of alleviating fuel-supply and other issues in power system planning. In reality, other technologies such as power-to-gas and natural gas storage can also alleviate these types of issues. Moreover, natural gas pipelines themselves provide a limited form of energy storage, insomuch as line pack can increase fuel availability. We do not consider such alternatives because our focus is on the co-ordinated planning of EES with other traditional electrical and natural gas resources. This focus is motivated by recent real-world developments in the state of California, which is grappling with limited natural gas storage and supply in the Los Angeles basin through the deployment of EES.

Acknowledgment

Thank you to Armin Sorooshian, the editors, and four reviewers for helpful suggestions, comments, and conversations.

References

[1] B. Zhao, A. J. Conejo, and R. Sioshansi, "Coordinated Expansion Planning of Natural Gas and Electric Power Systems," *IEEE Transactions on Power Systems*, vol. 33, pp. 3064–3075, May 2018.

[2] "Assessment of energy storage systems suitable for use by electric utilities," Electric Power Research Institute, Palo Alto, CA, USA, Tech. Rep. EPRI-EM-264, 1976.

[3] "EPRI-DOE Handbook for Energy Storage for Transmission and Distribution Applications," Electric Power Research Institute and the U.S. Department of Energy, Palo Alto, CA and Washington, DC, USA, Tech. Rep. 1001834, 2003.

[4] M. Dicorato, G. Forte, M. Pisani, and M. Trovato, "Planning and Operating Combined Wind-Storage System in Electricity Market," *IEEE Transactions on Sustainable Energy*, vol. 3, pp. 209–217, April 2012.

[5] N. Zhang, C. Kang, D. S. Kirschen, Q. Xia, W. Xi, J. Huang, and Q. Zhang, "Planning Pumped Storage Capacity for Wind Power Integration," *IEEE Transactions on Sustainable Energy*, vol. 4, pp. 393–401, April 2013.

[6] P. Xiong and C. Singh, "Optimal Planning of Storage in Power Systems Integrated With Wind Power Generation," *IEEE Transactions on Sustainable Energy*, vol. 7, pp. 232–240, January 2016.

[7] M. Sedghi, A. Ahmadian, and M. Aliakbar-Golkar, "Optimal Storage Planning in Active Distribution Network Considering Uncertainty of Wind Power Distributed Generation," *IEEE Transactions on Power Systems*, vol. 31, pp. 304–316, January 2016.

[8] S. W. Alnaser and L. F. Ochoa, "Optimal Sizing and Control of Energy Storage in Wind Power-Rich Distribution Networks," *IEEE Transactions on Power Systems*, vol. 31, pp. 2004–2013, May 2016.

[9] I. Miranda, N. Silva, and H. Leite, "A Holistic Approach to the Integration of Battery Energy Storage Systems in Island Electric Grids With High Wind Penetration," *IEEE Transactions on Sustainable Energy*, vol. 7, pp. 775–785, April 2016.

[10] B. Xu, Y. Wang, Y. Dvorkin, R. Fernández Blanco Carramolino, C. A. Silva-Monroy, J.-P. Watson, and D. S. Kirschen, "Scalable Planning for Energy Storage in Energy and Reserve Markets," *IEEE Transactions on Power Systems*, vol. 32, pp. 4515–4527, November 2017.

[11] Y. Dvorkin, R. Fernández Blanco Carramolino, Y. Wang, B. Xu, D. Kirschen, H. Pandžić, J.-P. Watson, and C. A. Silva-Monroy, "Co-planning of Investments in Transmission and Merchant Energy Storage," *IEEE Transactions on Power Systems*, vol. 33, pp. 245–256, January 2018.

[12] X. Shen, M. Shahidehpour, Y. Han, S. Zhu, and J. Zheng, "Expansion Planning of Active Distribution Networks With Centralized and Distributed Energy Storage Systems," *IEEE Transactions on Sustainable Energy*, vol. 8, pp. 126–134, January 2017.

[13] H. Alharbi and K. Bhattacharya, "Stochastic Optimal Planning of Battery Energy Storage Systems for Isolated Microgrids," *IEEE Transactions on Sustainable Energy*, vol. 9, pp. 211–227, January 2018.

[14] A. Anvari-Moghaddam, T. Dragicevic, L. Meng, B. Sun, and J. M. Guerrero, "Optimal Planning and Operation Management of a Ship Electrical Power System with Energy Storage System," in *42nd Annual Conference of the IEEE Industrial Electronics Society*. Florence, Italy: Institute of Electrical and Electronics Engineers, 23-26 October 2016.

[15] A. Clerici, E. Tironi, and F. Castelli-Dezza, "Multiport Converters and ESS on 3-kV DC Railway Lines: Case Study for Braking Energy Savings," *IEEE Transactions on Industry Applications*, vol. 54, pp. 2740–2750, May-June 2018.

[16] A. Lachuriya and R. D. Kulkarni, "Stationary Electrical Energy Storage Technology for Global Energy Sustainability: A Review," in *2017 International Conference on Nascent Technologies in Engineering*. Navi Mumbai, India: Institute of Electrical and Electronics Engineers, 27-28 January 2017.

[17] P. Zou, Q. Chen, Q. Xia, G. He, C. Kang, and A. J. Conejo, "Pool equilibria including strategic storage," *Applied Energy*, vol. 177, pp. 260–270, 1 September 2016.

[18] C. Unsihuay-Vila, J. W. Marangon-Lima, A. C. Zambroni de Souza, I. J. Perez-Arriaga, and P. P. Balestrassi, "A Model to Long-Term, Multiarea, Multistage, and Integrated Expansion Planning of Electricity and Natural Gas Systems," *IEEE Transactions on Power Systems*, vol. 25, pp. 1154–1168, May 2010.

[19] J. Qiu, Z. Y. Dong, J. H. Zhao, Y. Xu, Y. Zheng, C. Li, and K. P. Wong, "Multi-Stage Flexible Expansion Co-Planning Under Uncertainties in a Combined Electricity and Gas Market," *IEEE Transactions on Power Systems*, vol. 30, pp. 2119–2129, July 2015.

[20] F. Barati, H. Seifi, M. S. Sepasian, A. Nateghi, M. Shafie-khah, and J. P. S. Catalão, "Multi-Period Integrated Framework of Generation, Transmission, and Natural Gas Grid Expansion Planning for Large-Scale Systems," *IEEE Transactions on Power Systems*, vol. 30, pp. 2527–2537, September 2015.

[21] Q. Zeng, B. Zhang, J. Fang, and Z. Chen, "A bi-level programming for multistage co-expansion planning of the integrated gas and electricity system," *Applied Energy*, vol. 200, pp. 192–203, 15 August 2017.

[22] T. Ding, Y. Hu, and Z. Bie, "Multi-Stage Stochastic Programming with Nonanticipativity Constraints for Expansion of Combined Power and Natural Gas Systems," *IEEE Transactions on Power Systems*, vol. 33, pp. 317–328, January 2018.

[23] C. He, L. Wu, T. Liu, and Z. Bie, "Robust Co-optimization Planning of Interdependent Electricity and Natural Gas Systems with a Joint $N-1$ and Probabilistic Reliability Criterion," *IEEE Transactions on Power Systems*, vol. 33, pp. 2140–2154, March 2018.

[24] Y. Hu, Z. Bie, T. Ding, and Y. Lin, "An NSGA-II based multi-objective optimization for combined gas and electricity network expansion planning," *Applied Energy*, vol. 167, pp. 280–293, 1 April 2016.

[25] J. Qiu, H. Yang, Z. Y. Dong, J. H. Zhao, K. Meng, F. J. Luo, and K. P. Wong, "A Linear Programming Approach to Expansion Co-Planning in Gas and Electricity Markets," *IEEE Transactions on Power Systems*, vol. 31, pp. 3594–3606, September 2016.

[26] X. Zhang, M. Shahidehpour, A. S. Alabdulwahab, and A. Abusorrah, "Security-Constrained Co-Optimization Planning of Electricity and Natural Gas Transportation Infrastructures," *IEEE Transactions on Power Systems*, vol. 30, pp. 2984–2993, November 2015.

[27] C. Shao, M. Shahidehpour, X. Wang, X. Wang, and B. Wang, "Integrated Planning of Electricity and Natural Gas Transportation Systems for Enhancing the Power Grid Resilience," *IEEE Transactions on Power Systems*, vol. 32, pp. 4418–4429, November 2017.

[28] M. Chaudry, N. Jenkins, M. Qadrdan, and J. Wu, "Combined gas and electricity network expansion planning," *Applied Energy*, vol. 113, pp. 1171–1187, January 2014.

[29] J. Qiu, Z. Y. Dong, J. H. Zhao, K. Meng, Y. Zheng, and D. J. Hill, "Low Carbon Oriented Expansion Planning of Integrated Gas and Power Systems," *IEEE Transactions on Power Systems*, vol. 30, pp. 1035–1046, March 2015.

[30] Y. Liu, R. Sioshansi, and A. J. Conejo, "Multistage Stochastic Investment Planning with Multiscale Representation of Uncertainties and Decisions," *IEEE Transactions on Power Systems*, vol. 33, pp. 781–791, January 2018.

[31] J. Czyzyk, M. P. Mesnier, and J. J. More, "The NEOS Server," *IEEE Journal on Computational Science and Engineering*, vol. 5, pp. 68–75, July-September 1998.

Bining Zhao (S'16) received the B.S. degree in electrical engineering and automation from North China Electric Power University, Baoding, China, in 2014. She is currently working toward her Ph.D. degree in the Department of Electrical and Computer Engineering at The Ohio State University, Columbus, OH.

Antonio J. Conejo (F'04) received the M.S. degree from the Massachusetts Institute of Technology, Cambridge, MA, in 1987, and the Ph.D. degree from the Royal Institute of Technology, Stockholm, Sweden, in 1990.

He is currently a professor in the Department of Integrated Systems Engineering and the Department of Electrical and Computer Engineering, The Ohio State University, Columbus, OH. His research interests include control, operations, planning, economics and regulation of electric energy systems, as well as statistics and optimization theory and its applications.

Ramteen Sioshansi (M'11–SM'12) holds the B.A. degree in economics and applied mathematics and the M.S. and Ph.D. degrees in industrial engineering and operations research from the University of California, Berkeley, and an M.Sc. in econometrics and mathematical economics from The London School of Economics and Political Science.

He is a professor in the Department of Integrated Systems Engineering at The Ohio State University, Columbus, OH. His research focuses on renewable and sustainable energy system analysis and the design of restructured competitive electricity markets.